AGU PUBLICATIONS

Geophysical Research Letters

RESEARCH LETTER
10.1002/2017GL074120

Key Points:
- Ground motion in Osaka Basin during the Tohoku earthquake was unexpectedly large
- Surface-waves are locally amplified by structure differently than body waves
- Accounting for effects of structure in Osaka Basin on surface-waves explains anomalous extreme ground motions during the Tohoku earthquake

Supporting Information:
- Supporting Information S1

Correspondence to:
V. C. Tsai,
tsai@caltech.edu

Citation:
Tsai, V. C., D. C. Bowden, and H. Kanamori (2017), Explaining extreme ground motion in Osaka basin during the 2011 Tohoku earthquake, *Geophys. Res. Lett.*, *44*, doi:10.1002/2017GL074120.

Received 10 MAY 2017
Accepted 18 JUL 2017
Accepted article online 20 JUL 2017

Explaining extreme ground motion in Osaka basin during the 2011 Tohoku earthquake

Victor C. Tsai[1], Daniel C. Bowden[1], and Hiroo Kanamori[1]

[1]Seismological Laboratory, California Institute of Technology, Pasadena, California, USA

Abstract Despite being 770 km away from the epicenter, observed ground motions due to the Tohoku earthquake in the Osaka Basin were unexpectedly large, with an amplification of more than a factor of 20 compared to immediately outside the basin, and including 2.7 m peak-to-peak roof displacements at one high-rise building. The local ground motions exceeded expectations based on standard computations of site response by a factor of 3, predicted frequencies of peak acceleration were off by at least 50%, and such discrepancies have not yet been explained quantitatively. Here we show that utilizing semianalytic theory for surface-wave amplification, we are able to accurately predict both the amplitudes and frequencies of large ground amplification in the Osaka Basin using only knowledge of the local one-dimensional structure. Comparison between this simple prediction and observed amplification was not expected to be so favorable and suggests that simple one-dimensional surface-wave site amplification factors can be useful in the absence of full three-dimensional wave propagation simulations. Such surface-wave amplification factors can be included in addition to the standard measures of site-specific site amplification and should help explain strong ground motion variability in future large earthquakes that shake Osaka Basin and elsewhere in the world.

Plain Language Summary Using the local structure to predict surface-wave amplification accurately explains extreme ground motion amplification in Osaka Basin during the 2011 Tohoku earthquake, whereas such ground motions have been unsuccessfully modeled with standard measures of site amplification. The results demonstrate how necessary it is to include a measure of surface-wave amplification if one is to accurately predict earthquake ground motions. The approach can potentially be incorporated into new site-specific earthquake hazards analyses in nearly an identical way to which existing approaches to site amplification are already being used.

1. Introduction

The 2011 M9.1 Tohoku-Oki earthquake was one of the largest earthquakes to occur this century [*Simons et al.*, 2011; *Nettles et al.*, 2011] and caused ground motions that exceeded accelerations of 2 m/s^2 in Tohoku prefecture [*Kurahashi and Irikura*, 2011; *Irikura and Kurahashi*, 2012]. Surprisingly, the Tohoku earthquake also caused strong ground motions in Osaka Basin, 770 km away from the epicenter, the most populated area in western Japan [*Sato et al.*, 2012; *Iwata et al.*, 2016]. While it is well known that the Osaka Basin is a deep sedimentary basin that is expected to locally amplify earthquake ground motions [e.g., *Sato*, 1990; *Pratt et al.*, 2003; *Miyakoshi et al.*, 2013; *Yoshimoto and Takemura*, 2014], the estimated amplification based on standard site-specific vertically propagating shear-wave site amplification calculations [e.g., *Kanai*, 1952; *Satoh et al.*, 1995; *Thompson et al.*, 2012] severely underestimated the ground motions compared to what was observed. Perhaps most importantly, long-period ground motions (3–10 s) were amplified by a factor of more than 20 (Figures 1 and 2) and underestimated by a factor of 3 using standard predictions of site-specific site amplification (see Figure 3, blue line), leading to significantly stronger shaking of high-rise buildings than expected. The Sakishima building, in particular, which was instrumented from the ground to the top floor, had peak-to-peak roof displacements of 2.7 m, due to much larger long-period (~6 s) ground motions near the resonant frequency of the building than expected [*Kashima et al.*, 2012; *Kanamori*, 2014]. With the possibility of great earthquakes at the much closer Nankai and Tonankai subduction zones, the significant and as yet still unexplained underestimate of ground motion in the Osaka Basin due to the Tohoku earthquake is alarming and underscores the importance of better quantitative understanding how much ground motions are amplified there.

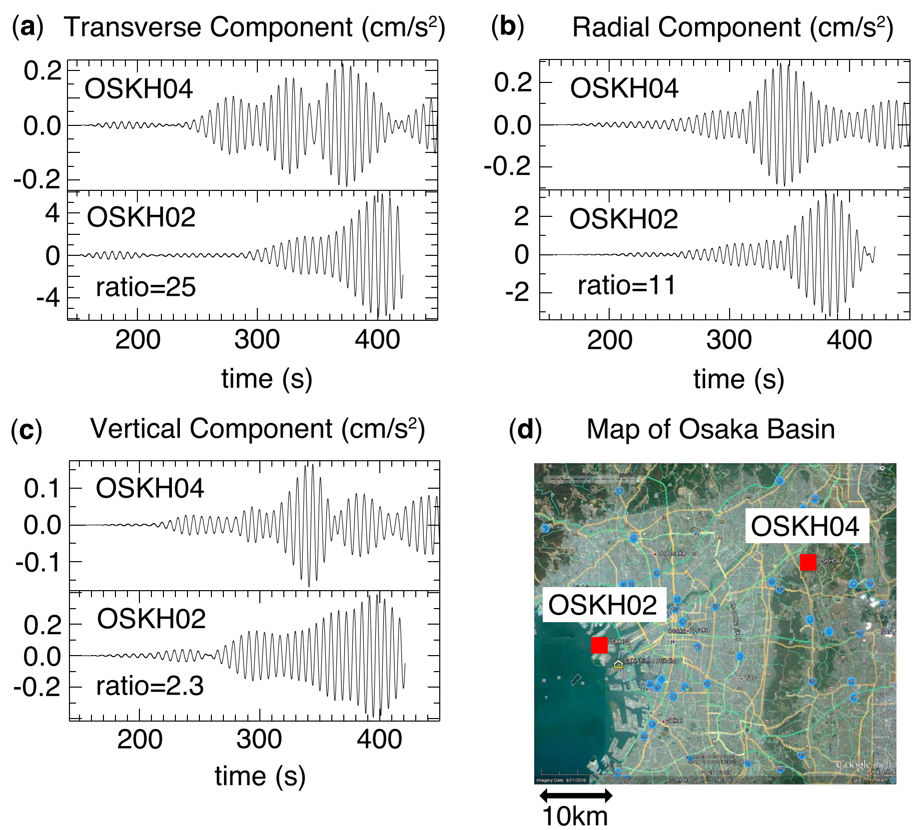

Figure 1. Seismic records from the Tohoku-Oki earthquake, filtered between 0.143 and 0.167 Hz (6–7 s, i.e., in the frequency range of peak amplification), observed at OSKH04 (upper panels) and OSKH02 (lower panels) for the (a) transverse, (b) radial, and (c) vertical components of motion. Ratios refer to the observed filtered peak amplitudes at OSKH02 divided by those at OSKH04. (d) Map of the Osaka Basin, showing stations OSKH02 and OSKH04.

2. Theory

Here we show that a simple semianalytical estimate of surface-wave amplification [*Bowden and Tsai*, 2017] adequately explains the amplification of ground motions in Osaka Basin. This estimate of amplification based on the local one-dimensional (1-D) velocity and density structure at a known site relative to the ground motion at a reference site of a different 1-D structure is similar in style to the site amplification calculations that are done by propagating shear waves vertically through a 1-D structure but explicitly accounts for surface-wave propagation rather than vertically incident shear-wave propagation. Such vertically propagating calculations of site amplification are currently used in some site-specific ground motion prediction equations (GMPEs) [e.g., *Cramer*, 2003; *McGuire and Toro*, 2008; *Stewart et al.*, 2014], but the estimate described here is for surface waves (both Love waves and Rayleigh waves) that propagate laterally (through a smoothly varying medium) rather than for vertically propagating shear waves. While such estimates will never be as accurate as those produced from a full three-dimensional (3-D) wave propagation simulation [e.g., *Bard and Bouchon*, 1980; *Olsen*, 2000; *Graves et al.*, 2010; *Iwaki and Iwata*, 2011], the simplicity of the calculation, the generality in which it can be utilized, the straightforward ability to evaluate one distinct cause of amplification, and the physical intuition that is gained from such a description makes it useful as an initial estimate.

Our calculation of surface-wave site amplification is based on the simple theory described by *Bowden and Tsai* [2017], which calculates the relative amplitudes of surface waves by imposing conservation of surface-wave energy flux (assuming no scattering). This assumption is a clear simplification of reality and specifically excludes the effect that lateral basin boundaries can have in reflecting waves and creating additional resonances but accounts for resonant-type behavior inherent in a 1-D (slow velocity) basin structure. The surface-wave site amplification term can be calculated as

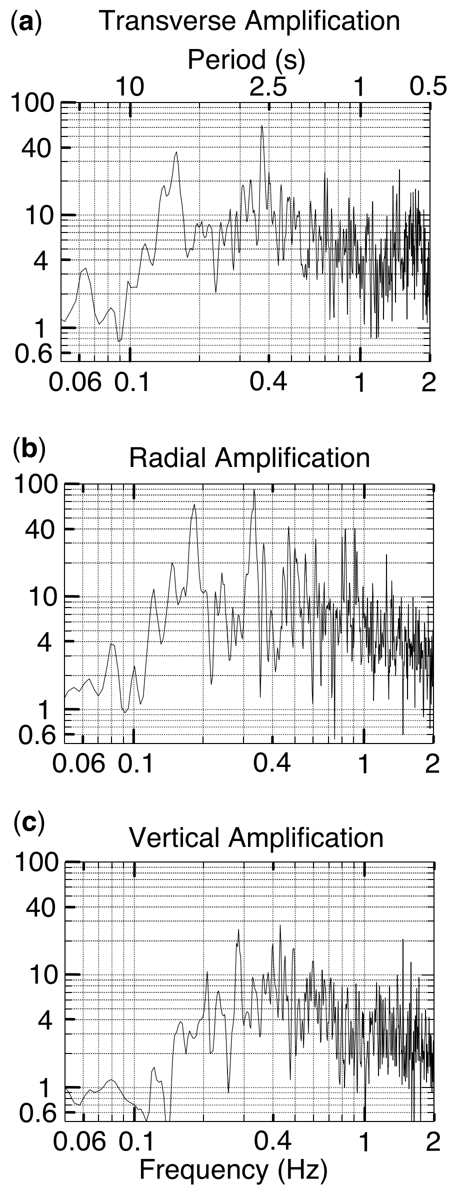

Figure 2. Observed spectral amplification ratios for OSKH02 relative to reference site OSKH04 from the Tohoku-Oki earthquake for the (a) transverse, (b) radial, and (c) vertical components of motion recorded from the Tohoku-Oki earthquake.

$$\frac{A}{A_R} = \frac{u(0)}{u_R(0)}\left(\frac{UI}{u_R I_R}\right)^{-1/2}, \quad (1)$$

where A/A_R is the surface wave amplitude at the site relative to a reference site, u(0) is the displacement eigenfunction at the surface, U is the group velocity, and I is the vertically integrated kinetic energy for the mode considered [*Tromp and Dahlen*, 1992]. Subscript R refers to the reference site, and the expression applies to any surface-wave component of motion. This result is derivable by observing that the surface-wave energy flux should be the group velocity multiplied by the average kinetic energy density [*Lighthill*, 1978; *Whitham*, 1999]. For Love waves, the average energy flux per unit width is then

$$F = \frac{U}{2}\int_0^\infty \frac{\rho}{2}\omega^2 A^2 u(z)^2 \mathrm{d}z = \frac{U\omega^2 A^2 I}{4}, \quad (2)$$

where ρ is density and ω is angular frequency, so that conservation of surface-wave energy flux requires equation (1) to hold (in the absence of geometric spreading). The derivation is similar for Rayleigh waves, but one must account for the two components of motion, and thus the general inclusion of u(0) in equation (1) (which is 1 for Love waves). These simple formulas have existed in the literature in various contexts for at least 50 years [*De Noyer*, 1961; *Woodhouse*, 1974; *Tromp and Dahlen*, 1992] but were only applied to ground motion hazards for the first time by *Bowden and Tsai* [2017].

Previous ground motion hazards work has noted that surface waves are amplified differently than direct *S* waves [e.g., *Pratt et al.*, 2003; *Arai and Tokimatsu*, 2005; *Furumura and Hayakawa*, 2007; *Miyakoshi et al.*, 2013; *Yoshimoto and Takemura*, 2014], but previous authors have not been able to calculate how potentially damaging surface-wave amplitudes are transformed solely due to surface-wave propagation from one 1-D structure (e.g., a reference structure) to another 1-D structure (e.g., within the basin of interest) and instead have assumed excitation and propagation of surface waves within a single 1-D structure (or have performed full 2-D/3-D simulations). As such, previous calculations of 1-D surface-wave amplification [e.g., *Miyakoshi et al.*, 2013; *Yoshimoto and Takemura*, 2014] do not allow one to compare the surface-wave amplitudes within a basin to amplitudes prior to entering the basin as is typically desired and which is accomplished with the theory of *Bowden and Tsai* [2017]. Finally, we note that the theory relied on is more general than the elliptical valley theory of *Trifunac* [1971] and accounts for both Rayleigh and Love waves rather than just incident SH waves.

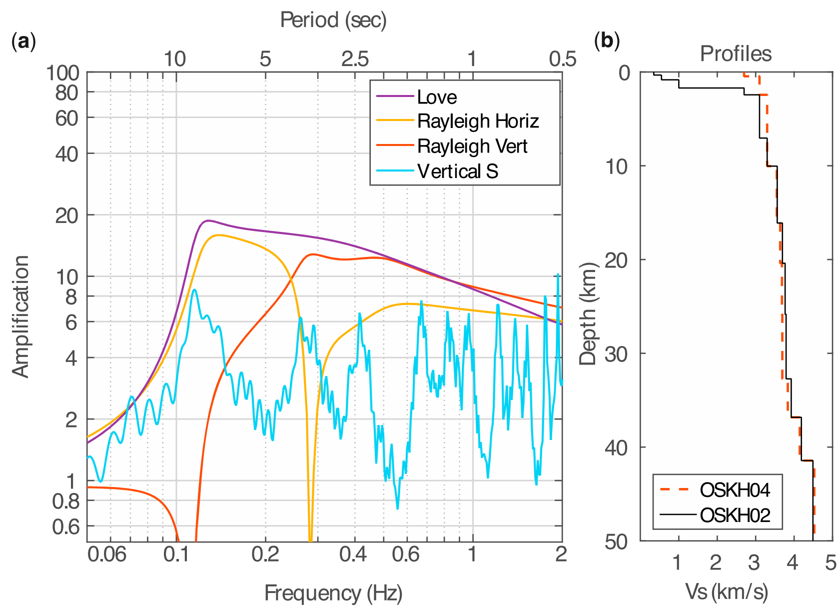

Figure 3. (a) Predicted spectral amplification ratios for OSKH02 relative to reference site OSKH04 for the three fundamental-mode surface wave components (Love in purple, horizontal-component Rayleigh in yellow, and vertical-component Rayleigh in red) as well as for the standard vertically propagating shear wave (in blue). (b) One-dimensional velocity profiles for OSKH02 (solid black) and OSKH04 (dashed red) used for the predictions shown in Figure 3a.

3. Results

Application of this theory to fundamental-mode Love waves (transversely polarized shear waves) and Rayleigh waves (vertical and longitudinal polarizations) in the Osaka Basin is shown in Figure 3. We use structure at the OSKH02 site in the middle of the Osaka Basin as the site of interest and structure at the OSKH04 site just outside the Osaka Basin as the reference site [*Fujiwara et al.*, 2009; *Japan Seismic Hazard Information Station*, 2017] to compute the three components of surface-wave site amplification. OSKH02 and OSKH04 are at azimuths of 243 and 242° relative to the Tohoku earthquake epicenter, respectively, and separated by approximately 30 km. As shown, the peak Love-wave amplification is approximately 20 at periods of 6–8 s, with a broader range of periods (1.3–9 s) that also have significant amplification. The Rayleigh-wave amplification is also large, with both the vertical and horizontal components reaching amplification factors above 10 in the 1–10 s period range. For comparison, the "standard" site amplification factor for the same pair of sites due to vertically propagating shear waves is also shown in Figure 3, which has maximum amplifications of only 6. It is clear from this comparison that while the standard site amplification factor cannot explain the large ground motions shown in Figure 2a that were amplified by a factor of 20, the Love-wave site amplification approximately explains both the amplitude and period of the observed ground motions, despite the simplicity of the calculation. While the roughness of the observed spectra, including the sharpness of the 6–8 s spectral peak, is not reproduced by the surface-wave predictions, which display a broader and smoother amplification spectrum, the simple predictions do a surprisingly good job at fitting a smoothed version of the observed spectra. (The observed roughness may be due to complexities in wave propagation that are not accounted for.) Moreover, the other components of motion (Figures 1b and 1c) are also approximately explained by the Rayleigh-wave site amplification terms, with observed spectral amplifications of nearly 20 on the other components (Figures 2b and 2c), and a higher frequency of maximum amplification on the vertical compared to horizontal component. It may also be noted that both the surface-wave and standard site amplification terms could be improved by using improved 1-D velocity structures. For example, it is well known that the standard site amplification peak can be moved to a more realistic period of 6.5 s from the peak at 8 s with slight modifications to the velocity structure [*Iwaki and Iwata*, 2011; *Asano et al.*, 2016].

While not the focus of this contribution, we note that the simple analytic theory described here for estimating surface-wave amplification also explains much of the long-period (3–15 s) amplification observed in other sedimentary basins (see supporting information), including amplification of the 2004 Chuetsu (Niigata) earthquake in the Kanto Basin [*Furumura and Hayakawa*, 2007; *Denolle et al.*, 2014; *Kennett et al*., 1995] and amplification of the 2010 El Mayor-Cucapah earthquake in the Los Angeles Basin [*Bowden and Tsai*, 2017; *Lee et al*., 2014]. Thus, while some of the observed amplification may be attributed to other effects, such as lateral scattering and complex basin reflections, a considerable fraction can be attributed directly to the 1-D surface-wave effect described here. Finally, we note that higher-order mode contributions can also be calculated (see supporting information).

4. Conclusions

We have shown that a simple semianalytical theory for surface-wave amplification adequately explains the extreme amplifications of a factor of 20 in the Osaka Basin, while standard measures of site-specific site amplification do not. As such, these 1-D surface-wave site amplification factors are of clear use for earthquake hazards prediction, and the simplicity with which such factors can be computed allows them to potentially be included in site-specific GMPEs without needing to perform a full 3-D seismic wave propagation simulation. Applications of such corrections to earthquake ground motion predictions in the Osaka Basin and elsewhere are crucial particularly due to the possibility of future regional megathrust earthquakes that will have strong surface waves.

Acknowledgments
We thank T. Furumura and two anonymous reviewers for comments that helped improve the manuscript. The KiK-net data used in this study were obtained from the National Research Institute for Earth Science and Disaster Prevention (NIED) data centers, http://www.kyoshin.bosai.go.jp/kyoshin/. This work was partially supported by NSF EAR-1453263.

References

Arai, H., and K. Tokimatsu (2005), S-wave velocity profiling by joint inversion of microtremor dispersion curve and horizontal-to-vertical (H/V) spectrum, *Bull. Seismol. Soc. Am.*, *95*, 1766–1778.

Asano, K., H. Sekiguchi, T. Iwata, M. Yoshimi, T. Hayashida, H. Saomoto, and H. Horikawa (2016), Modelling of wave propagation and attenuation in the Osaka sedimentary basin, western Japan, during the 2013 Awaji Island earthquake, *Geophys. J. Int.*, *204*, 1678–1694.

Bard, P.-Y., and M. Bouchon (1980), The seismic response of sediment-filled valleys. Part 1. The case of incident SH waves, *Bull. Seismol. Soc. Am.*, *70*, 1263–1286.

Bowden, D. C., and V. C. Tsai (2017), Earthquake ground motion amplification for surface waves, *Geophys. Res. Lett.*, *44*, 121–127, doi:10.1002/2016GL071885.

Cramer, C. H. (2003), Site-specific seismic-hazard analysis that is completely probabilistic, *Bull. Seismol. Soc. Am.*, *93*, 1841–1846.

De Noyer, J. (1961), The effect of variations in layer thickness on Love waves, *Bull. Seismol. Soc. Am.*, *51*, 227–235.

Denolle, M. A., H. Miyake, S. Nakagawa, N. Hirata, and G. C. Beroza (2014), Long-period seismic amplification in the Kanto Basin from the ambient seismic field, *Geophys. Res. Lett.*, *41*, 2319–2325, doi:10.1002/2014GL059425.

Fujiwara, H., et al. (2009), A study on subsurface structure model for deep sedimentary layers of Japan for strong-motion evaluation [in Japanese], Technical note 337, National Research Institute for Earth Science and Disaster Prevention, Tsukuba, Japan.

Furumura, T., and T. Hayakawa (2007), Anomalous propagation of long-period ground motions recorded in Tokyo during the 23 October 2004 M_w 6.6 Niigata-ken Chuetsu, Japan, earthquake, *Bull. Seismol. Soc. Am.*, *97*, 863–880.

Graves, R., et al. (2010), CyberShake: A physics-based seismic hazard model for southern California, *Pure Appl. Geophys.*, *168*, 367–381.

Irikura, K., and S. Kurahashi (2012), High acceleration motions generated from the 2011 Pacific coast off Tohoku, Japan earthquake, Proceedings of the Fifteenth World Conference on Earthquake Engineering, Lisbon.

Iwaki, A., and T. Iwata (2011), Estimation of three-dimensional boundary shape of the Osaka sedimentary basin by waveform inversion, *Geophys. J. Int.*, *186*, 1255–1278.

Iwata, T., H. Kubo, K. Asano, K. Sato, and S. Aoi (2016), Long-period ground motion characteristics and simulations in the Osaka Basin during the 2011 Great Tohoku Earthquake, 5th IASPEI/IAEE International Symposium: Effects of Surface Geology on Seismic Motion, Taipei.

Japan Seismic Hazard Information Station (2017), Webpage for the Japan seismic hazard information station. [Available at http://www.j-shis.bosai.go.jp/map/JSHIS2/download.html?lang=en, website accessed February 2017.]

Kanai, K. (1952), Relation between the nature of surface layer and the amplitudes of earthquake motions, *Bull. Earthquake Res. Inst.*, *30*, 31–37.

Kanamori, H. (2014), The diversity of large earthquakes and its implication for hazard mitigation, *Annu. Rev. Earth Planet. Sci.*, *42*, 7–26.

Kashima, T., S. Koyama, and I. Okawa (2012), Strong motion records in buildings from the 2011 off the Pacific coast of Tohoku earthquake, *Build. Res. Data No. 135*, Build. Res. Inst. Tsukuba, Japan.

Kennett, B. L. N., E. R. Engdahl, and R. Buland (1995), Constraints on seismic velocities in the earth from traveltimes, *Geophys. J. Int.*, *122*, 108–124.

Kurahashi, S., and K. Irikura (2011), Source model for generating strong ground motions during the 2011 off the Pacific coast of Tohoku earthquake, *Earth Planets Space*, *63*, 571–576.

Lee, E., P. Chen, T. H. Jordan, P. B. Maechling, M. A. M. Denolle, and G. C. Beroza (2014), Full 3-D tomography for crustal structure in Southern California based on the scattering-integral and the adjoint-wavefield methods, *J. Geophys. Res. Solid Earth*, *119*, 6421–6451, doi:10.1002/2014JB011346.

Lighthill, M. J. (1978), *Waves in Fluids*, Cambridge Univ. Press, Cambridge.

McGuire, R. K., and G. R. Toro (2008), Site-specific seismic hazard analysis, 14th World Conference on Earthquake Engineering, Beijing, 12–17 Oct.

Miyakoshi, K., M. Horike, and R. Nakamiya (2013), Long predominant period map and detection of resonant high-rise buildings in the Osaka Basin, western Japan, *Bull. Seismol. Soc. Am.*, *103*, 247–257.

Nettles, M., G. Ekstrom, and H. C. Koss (2011), Centroid-moment-tensor analysis of the 2011 off the Pacific coast of Tohoku Earthquake and its larger foreshocks and aftershocks, *Earth Planets Space*, *63*, 519–523.

Olsen, K. B. (2000), Site amplification in the Los Angeles Basin from three-dimensional modeling of ground motion, *Bull. Seismol. Soc. Am.*, *90*, S77–S94.

Pratt, T. L., T. M. Brocher, C. S. Weaver, K. C. Creager, C. M. Snelson, R. S. Crosson, K. C. Miller, and A. M. Trehu (2003), Amplification of seismic waves by the Seattle Basin, Washington state, *Bull. Seismol. Soc. Am.*, *93*, 533–545.

Sato, T. (1990), Simulation of observed seismograms on sedimentary basin using theoretical seismograms in the period range from 2 to 20 s—Synthesis of seismograms at Kobe and Osaka stations for the 1961 Kita-Mino earthquake, *JEES*, *33*, 193–198.

Sato, K., K. Asano, and T. Iwata (2012), Long-period ground motion characteristics of the Osaka Sedimentary Basin during the 2011 Great Tohoku Earthquake, Proceedings of the Fifteenth World Conference on Earthquake Engineering, Lisbon.

Satoh, T., H. Kawase, and T. Sato (1995), Evaluation of local site effects and their removal from borehole records observed in the Sendai region, Japan, *Bull. Seismol. Soc. Am.*, *85*, 1770–1789.

Simons, M., et al. (2011), The 2011 magnitude 9.0 Tohoku-Oki earthquake: Mosaicking the megathrust from seconds to centuries, *Science*, *332*, 1421–1425, doi:10.1126/science.1206731.

Stewart, J.P., K. Afshari, and Y.M.A. Hashash (2014), Guidelines for performing hazard-consistent one-dimensional ground response analysis for ground motion prediction, Pacific Earthquake Engineering Research Center Report.

Thompson, E. M., L. G. Baise, Y. Tanaka, and R. E. Kayen (2012), A taxonomy of site response complexity, *Soil Dyn. Earthquake Eng.*, *41*, 32–43.

Trifunac, M. D. (1971), Surface motion of a semi-cylindrical alluvial valley for incident plane SH waves, *Bull. Seismol. Soc. Am.*, *61*, 1755–1770.

Tromp, J., and F. A. Dahlen (1992), Variational principles for surface wave propagation on a laterally heterogeneous earth – II. Frequency-domain JWKB theory, *Geophys. J. Int.*, *109*, 599–619.

Whitham, G. B. (1999), *Linear and Nonlinear Waves*, John Wiley, Hoboken, N. J.

Woodhouse, J. H. (1974), Surface waves in a laterally varying layered structure, *Geophys. J. R. Astron. Soc.*, *37*, 461–490.

Yoshimoto, K., and S. Takemura (2014), A study on the predominant period of long-period ground motions in the Kanto Basin, Japan, *Earth Planets Space*, *66*, 100, doi:10.1186/1880-5981-66-100.

AGU PUBLICATIONS

Geophysical Research Letters

Supporting Information for

Explaining Extreme Ground Motion in Osaka Basin during the 2011 Tohoku Earthquake

Victor C. Tsai[1], Daniel C. Bowden[1], and Hiroo Kanamori[1]

[1] Seismological Laboratory, California Institute of Technology, Pasadena, CA 91125, USA.

Contents of this file

Figures S1 to S3

Introduction

This supporting document contains 3 figures, all of which describe synthetic calculations for surface-wave amplification in different situations. The first figure (Figure S1) describes surface-wave amplification predictions for a simplified basin (layer over a halfspace) geometry, including predictions for higher-order Love and Rayleigh waves. The second figure (Figure S2) describes surface-wave amplification predictions for the Kanto Basin, using the simple structure from Figure 5 of *Furumura and Hayakawa [2007]* for station SIT009 within the Kanto Basin as the site of interest, and using the model AK135 *[Kennett et al., 1995]* as the reference structure. The third figure (Figure S3) describes surface-wave amplification predictions for the Los Angeles Basin, using structure from the SCEC CVM-S4.26 *[Lee et al., 2014]* at station USC within the Los Angeles Basin as the site of interest, and using structure from the SCEC CVM at station PASC as the reference structure.

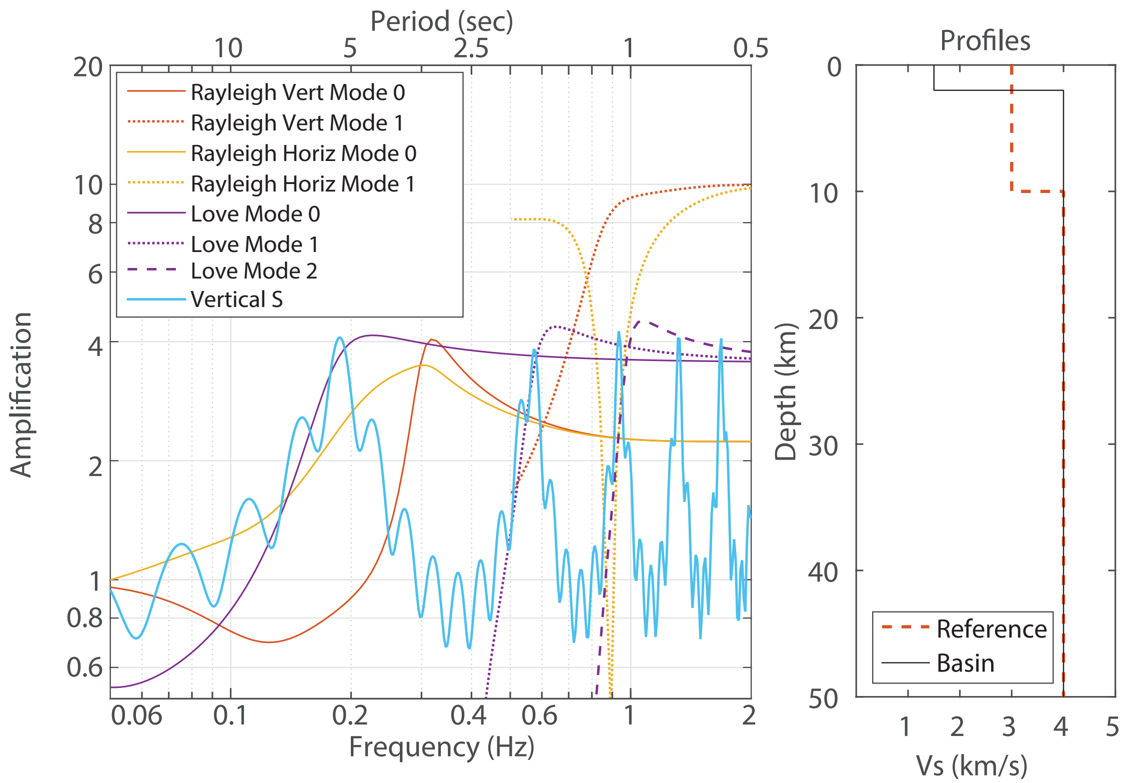

Figure S1. (a) Predicted spectral amplification ratios for a simplified basin geometry. Both the site of interest and the reference site structures are taken to be layers over a halfspace, with the shallow basin site having a much slower shear wave velocity (1.5 km/s; 2-km basin depth) compared to the reference site (3.0 km/s; 10-km basin depth). Predictions are for the three fundamental-mode ('mode 0') surface-wave components (Love in purple, horizontal-component Rayleigh in yellow, and vertical-component Rayleigh in red), the 'standard' vertically-propagating shear wave (in blue), the first higher-order ('mode 1') surface-wave components (same colors as for the fundamental mode, but with dotted lines instead of solid lines), and the second higher-order ('mode 2') Love wave (dashed purple). It may be noted that the frequencies at which the first and second higher-order Love waves begin to be amplified correspond approximately with the frequencies of the second and third resonance peaks of the vertically-propagating shear wave, respectively, as expected. At low frequencies, the higher-order Rayleigh-mode computations are unstable and are not plotted. **(b)** One-dimensional velocity profiles for the 'basin' site (solid black) and 'reference' site (dashed red) used for the predictions shown in panel (**a**).

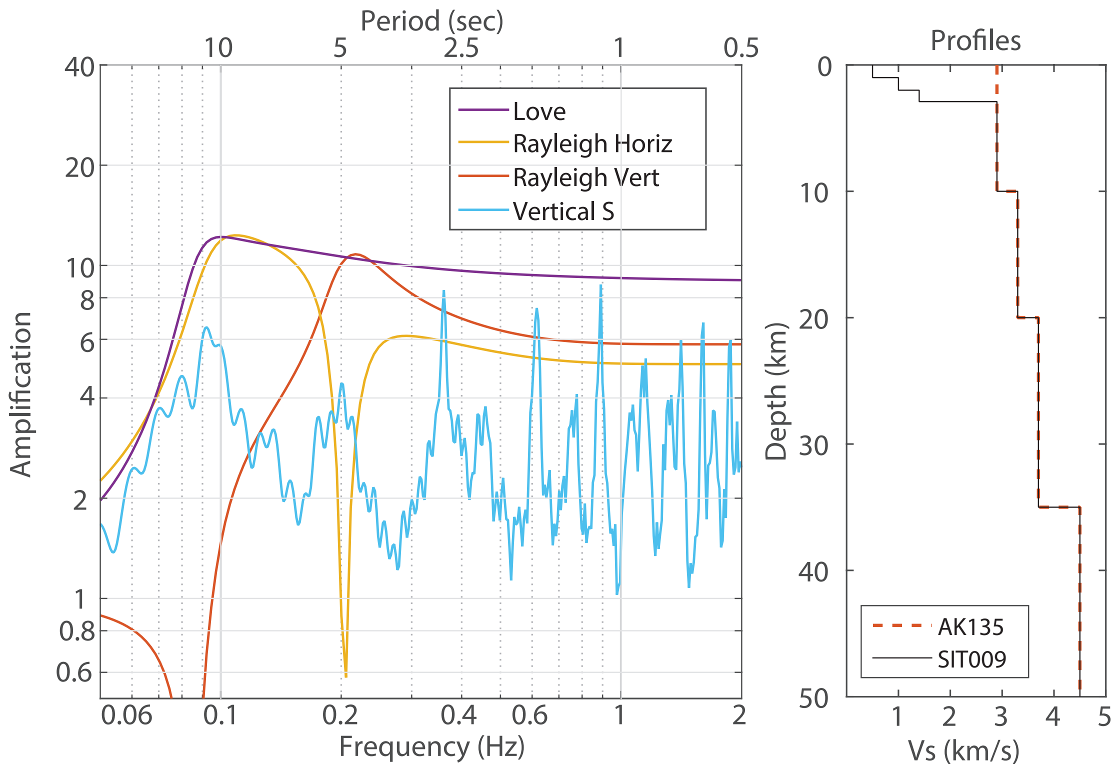

Figure S2. (a) Predicted spectral amplification ratios for SIT009 relative to reference structure AK135 *[Kennett et al., 1995]*. Predictions are for the three fundamental-mode surface-wave components (Love in purple, horizontal-component Rayleigh in yellow, and vertical-component Rayleigh in red) as well as for the 'standard' vertically-propagating shear wave (in blue). The predicted Love and Rayleigh amplification ratios can explain a significant fraction of the observed amplification of the 2004 Chuetsu (Niigata) Earthquake observed in the Kanto Basin by *Furumura and Hayakawa [2007]*. **(b)** One-dimensional velocity profiles for SIT009 (solid black) and AK135 (dashed red) used for the predictions shown in panel (**a**). Note that AK135 is used also for SIT009 at depths below the Kanto Basin, as described by *Furumura and Hayakawa [2007]*.

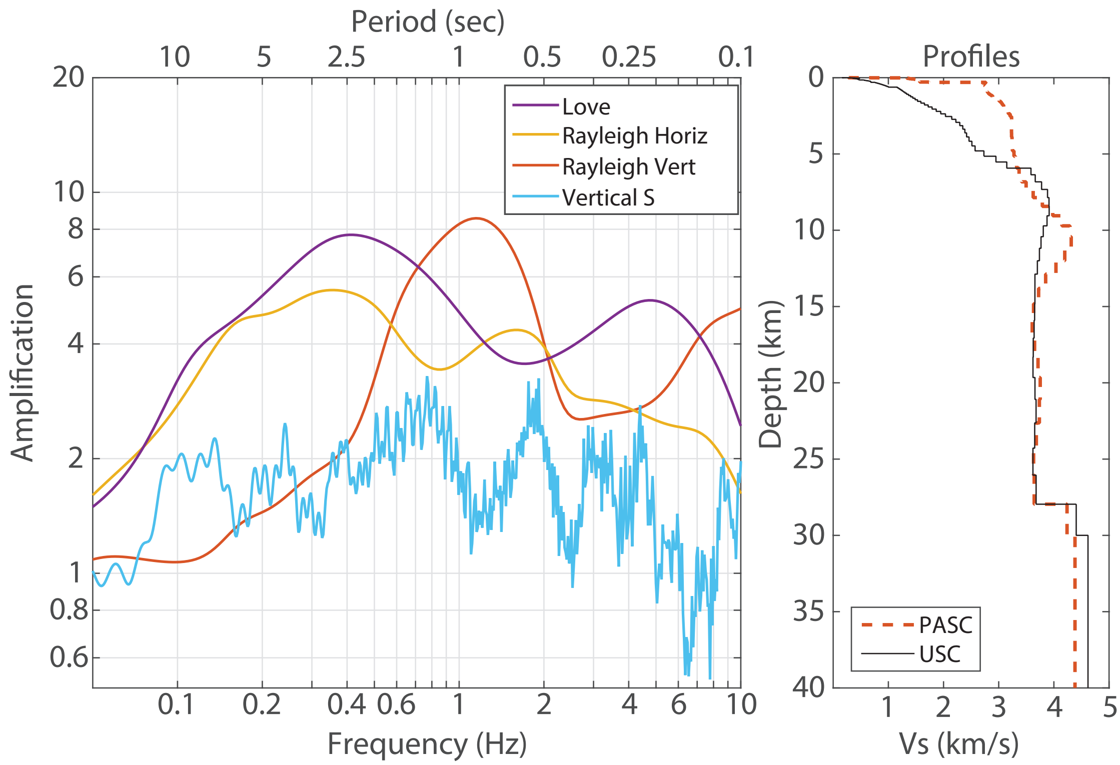

Figure S3. (a) Predicted spectral amplification ratios for USC relative to reference site PASC. Predictions are for the three fundamental-mode surface-wave components (Love in purple, horizontal-component Rayleigh in yellow, and vertical-component Rayleigh in red) as well as for the 'standard' vertically-propagating shear wave (in blue). The predicted Love and Rayleigh amplification ratios can explain a significant fraction of the observed amplification of the 2010 El Mayor-Cucapah Eathquake observed in the Los Angeles Basin [*Bowden and Tsai, 2017*]. **(b)** One-dimensional velocity profiles for USC (solid black) and PASC (dashed red) used for the predictions shown in panel (**a**). Note that both structures are taken from the SCEC CVM-S4.26 *[Lee et al., 2014]*.